



**Michigan
Technological
University**

Michigan Technological University
Digital Commons @ Michigan Tech

Department of Physics Publications

Department of Physics

3-1-1998

The texture of clouds

A. R. Jameson
RJH Scientific, Inc.

Alexander Kostinski
Michigan Technological University

R A. Black
Atlantic Oceanographic and Meteorological Laborator


Follow this and additional works at: <https://digitalcommons.mtu.edu/physics-fp>

 Part of the [Physics Commons](#)

Recommended Citation

Jameson, A. R., Kostinski, A., & Black, R. A. (1998). The texture of clouds. *Journal of Geophysical Research*, 103(D6), 6211-6219. <http://dx.doi.org/10.1029/98JD00081>
Retrieved from: <https://digitalcommons.mtu.edu/physics-fp/240>

Follow this and additional works at: <https://digitalcommons.mtu.edu/physics-fp>

 Part of the [Physics Commons](#)

The texture of clouds

A. R. Jameson

RJH Scientific, Inc., Alexandria, Virginia

A. B. Kostinski

Department of Physics, Michigan Technological University, Houghton

R. A. Black

National Oceanic and Atmospheric Administration, Atlantic Oceanographic and Meteorological Laboratory, Miami, Florida

Abstract. Using a precise definition of clustering, it is shown that in two tropical cumulus clouds, droplets appear to be bunched over distances ranging from at least a kilometer or more down to several centimeters. A statistical framework is proposed for quantifying clustering in terms of a Poisson probability mixture. While these observations require further substantiation in many different clouds, droplet clustering may play a role in diverse phenomena from the coalescence growth of raindrops to the scattering of radiation by clouds.

1. Introduction

It is widely assumed that cloud droplets are distributed in space as evenly as randomness permits, i.e., in accordance with Poisson statistics [Cornford, 1967; Rogers and Yau, 1989, p. 134; Young, 1993, p. 181]. This is not an innocuous assumption, however. Current understanding of how cloud droplets evolve into rain and our knowledge of the radiative properties of clouds are based upon an assumption of a Poisson distribution of droplets. Even within the Poissonian constraint, however, it was realized that the spatial distribution of droplets is “even” only in an “average” sense and that “randomness” produces fluctuations in the droplet concentrations from one location to another [Telford, 1955]. This simple concept appeared to explain the more rapid coalescence of droplets into rain than could be understood using calculations based upon deterministic droplet concentrations [Telford, 1955; Twomey, 1964]. Nevertheless, it was demonstrated in subsequent stochastic collision-coalescence calculations that such fluctuations, if Poissonian, were too small to have any significant effect [Gillespie, 1972, 1975] on the speed of raindrop evolution. To quote Young [1993, p. 185],

It may be concluded that the differences due to the stochastic nature of the collection processes are negligible and that the cloud behavior may be adequately described by the quasistochastic treatment.

However, what would happen if concentration fluctuations (i.e., variances) were super-Poissonian?

Using holographic measurements in fog, Kozikowska *et al.* [1984] found that the mean distance between droplets showed no evidence of significant droplet clustering or deviations from Poisson statistics. On the other hand, in convective cumulus clouds, Paluch and Baumgardner [1986] found evidence of “patchy mixing” and clustering on scales of 10 m and less. Using forward scattering optical cloud probes, Baker [1992]

reported non-Poissonian deviations in convective cumulus clouds even down to scales of several centimeters, an effect he attributed to small-scale turbulence. These results suggest that on scales of several centimeters to several meters, droplet clustering associated with deviations from a Poisson distribution may occur in the turbulent environments of convective clouds. However, such conclusions are still considered far from proven by many cloud physicists (see the discussion by Pruppacher and Klett [1997, pp. 27–30], and no stochastic framework for describing clustering appears in the cloud physics literature.

Moreover, because cloud physicists are still primarily concerned with clustering on very small scales, the question of clustering on longer scales remains open to study. Yet, clustering on longer scales may affect other cloud properties. For example, the optical density of clouds can be characterized by the mean free path of a photon, typically of the order of several tens to hundreds of meters. These scales, then, are the ones most relevant to cloud radiation [Cahalan, 1989]. Indeed, it appears that the radiative properties of clouds may depend upon how the droplets are distributed in space [e.g., Cahalan *et al.*, 1994]. If so, a knowledge of the spatial distribution of cloud droplets may become important for illuminating the enigmatic role clouds play in the radiation budget of the Earth [Ramanathan *et al.*, 1995].

As a step toward addressing such questions, the much more modest objective of this paper is simply to explore further the spatial structure of droplet concentrations in clouds by comparing our results with previous observations and by extending observations to longer scales. It is shown below that in conflict with a Poisson distribution, droplets in two tropical cumulus clouds are often “clustered” apparently on many scales. A statistical framework is proposed for describing such clustering.

2. What Is Clustering?

To begin, however, it is first necessary to give a precise definition of what is meant by “clustering.” (The reader is referred to Kostinski and Jameson [1997] for a more detailed discussion.) Clustering is found over a wide range of physical

Copyright 1998 by the American Geophysical Union.

Paper number 98JD00081.
0148-0227/98/98JD-00081\$09.00

phenomena. In all cases, clustering is identified as deviations from expectations for a Poisson distribution.

This is not by accident because the Poisson distribution permits the uniform, completely uncorrelated, random distribution of events (in this case, droplets in space). One of the assumptions behind the Poisson distribution is that counts (events) in nonoverlapping volumes (time intervals) are statistically independent. Using the two-point correlation function, *Kostinski and Jameson* [1997] show that it is the violation of this condition that leads to deviations from the Poisson distribution and therefore to the clustering of raindrops. A more physical interpretation of this discussion is given below.

If clustering exists, it must be demonstrated that physical variations in concentration (number per unit volume) exceed those anticipated for a Poisson distribution, as discussed above. Specifically, to see if cloud droplets are clustered, one begins with the product of the number of droplets in two identical volumes separated by a fixed distance ξ and then subtracts the square of the average value computed over the entire volume under study, \mathcal{V} , for an ensemble of several such pairs in \mathcal{V} . That is, let us consider the quantity

$$\phi(\xi) = \langle k(0)k(\xi) \rangle - \mu^2 \quad (1)$$

where $k(0)$ and $k(\xi)$ are the number of droplets in two identical volumes separated by distance ξ , μ is the mean number over all of \mathcal{V} , and the angle brackets denote an ensemble average. If the number of droplets in \mathcal{V} is distributed evenly on average, then $\langle k(0)k(\xi) \rangle = \mu^2$ so that $\phi(\xi) = 0$. If, on the other hand, there were an “excess” number of droplets in volumes separated by scales of ξ on average (because of intermittent turbulence, for example), $\phi(\xi)$ would not equal zero; that is, $[\langle k(0)k(\xi) \rangle \neq \mu^2]$. In other words, there would be a clustering of droplets compared to the average number expected for a uniform, statistical spatial (Poisson) distribution over \mathcal{V} .

The statistical interpretation of (1) given by *Kostinski and Jameson* [1997] is in terms of the excess two-point correlation function given by

$$\eta(\xi) \equiv \frac{[\langle k(0)k(\xi) \rangle - \mu^2]}{\mu^2} = \frac{\langle k(0)k(\xi) \rangle}{\mu^2} - 1 \quad (2)$$

For a Poisson distribution, $k(0)$ and $k(\xi)$ would be statistically independent. Consequently, $\langle k(0)k(\xi) \rangle = \mu^2$ and $\eta(\xi) = 0$ even though k fluctuates from location to location. However, when $\eta(\xi) \neq 0$, there is correlation. Hence according to *Kostinski and Jameson* [1997], it is the statistical correlation of cloud droplets in one volume on the presence of droplets in another that distinguish clustering from a uniform Poisson distribution. It is likely that intermittent convection and turbulence, as well as other factors, lead to the cloud droplet bunching. Results are given below for aircraft measurements in two tropical cumulus clouds.

3. Observations of Clustering

During the Tropical Ocean-Global Atmosphere/Coupled Ocean-Atmosphere Response Experiment (TOGA/COARE) in 1992–1993, the Electra aircraft operated by the National Center for Atmospheric Research (NCAR) flew (at a nominal air speed of about 130 m s^{-1}) in a nearly saturated environment about 3 km above ground level (agl) or about 1 km above the cloud base through precipitating warm tropical clouds.

Cloud and precipitation particles were observed using the Particle Measuring System, Inc. (PMS) two-dimensional (2-D) optical array probes [*Knollenberg*, 1981]. For this study, droplets from 0.025 to 0.80 mm diameter were imaged using the PMS 2D-C instrument and were averaged over 1 s, yielding a count in a sample volume of about 1 L over a 130 m flight path. While slight differences in sampling volume as functions of drop size were taken into account, all the analyses (with one minor exception) were performed on 50 μm diameter drop counts rendering such volume differences irrelevant. Moreover, absolute concentrations are not critical to this statistical study.

Other errors can occur, however. Occasionally, the size of a few drops can be miscalculated so that they may be erroneously included in the count at a particular size bin. On the other hand, others of the correct size, which should be included, are sometimes excluded. While we do not know the precise frequency of such missizing, based upon the extensive experience and persistent use of this instrument, it seems unlikely that measurements over the entire wide range of scales considered in this study are significantly affected.

Two examples of 130 m resolution time series measurements for 50 μm diameter drops are shown in Figure 1. As with any stochastic meteorological structure, there are substantial fluctuations. The true variability is likely to be larger than illustrated in the data, however, because of instrument effects. One such effect is the so-called “dead time,” arising when data are being transferred from a buffer to storage. A second is caused by so-called “streakers,” i.e., accumulated water peeling off the leading edge of the probes as intermittent sheets of water. In these data, streakers were removed, but during that interval, an observation of real droplets is also lost. The net effect is to create approximately uniformly interspersed data gaps. This, in turn, leads to a loss of information and therefore to a decrease in correlation among samples. Hence any evidence of correlation and clustering appearing in the analyses should be a conservative reflection of actual non-Poissonian deviations.

The two-point correlation function given by (2) is illustrated in Figure 2a for 50 μm diameter drops and in Figure 2b for the total number of droplets (25–800 μm) detected by this probe in these two clouds. In both clouds, correlated clustering is evident at scales less than 500–1000 m down to the smallest resolution of these data (130 m).

While (2) is useful for determining the overall structure of clustering, it is worth looking in greater detail both at scales larger than 500 m and at smaller than 130 m. At the larger end, the well-known property of the Poisson distribution that the variance and mean are equal [e.g., *Feller*, 1968, p. 228; *Ochi*, 1990, p. 47] is used to detect deviations associated with clustering by computing the ratio of the observed variance to that anticipated for an “equivalent” ($\sigma^2 = \mu$) Poisson distribution. This technique has a spatial (temporal) resolution determined by the data rate and the size of the data window, i.e., the number of samples used to compute the means and variances. (While this technique was developed independently by *Jameson and Kostinski* [1998] for their studies of rain, it turns out that a more complex version of this idea was developed earlier as the “Fishing test” by *Baker* [1992] for his cloud studies. Interestingly, as early as 1934, Hubble used this variance test to explore galaxy counts [*Peebles*, 1980, p. 138].) Figure 3 indicates that on scales from 0.8 to 2.1 km in these clouds, non-Poisson statistics appear at many locations in such “windowed” data.

To study smaller scales, interdrop distances (times) between events (droplets) are used. While suggested originally for cloud studies by Baumgardner [1986], this approach has been used extensively in other branches of physics as well [van Kampen, 1992, p. 44]. For a Poisson process, the distribution of interdrop distances is given by [Ochi, 1990, p. 432]

$$P(\xi)d\xi = \frac{1}{\bar{\xi}} \exp\left(-\frac{\xi}{\bar{\xi}}\right) d\xi \quad (3)$$

where $P(\xi)d\xi$ is the probability of encountering exactly no droplets during distance ξ , and $\bar{\xi}$ is the mean distance between successive drops. (This distribution, however, only applies to a one-dimensional, straight-line pass.) Consequently, deviations of the observed distribution from exponential indicate a non-Poisson spatial distribution of cloud droplets. Note that in (3)

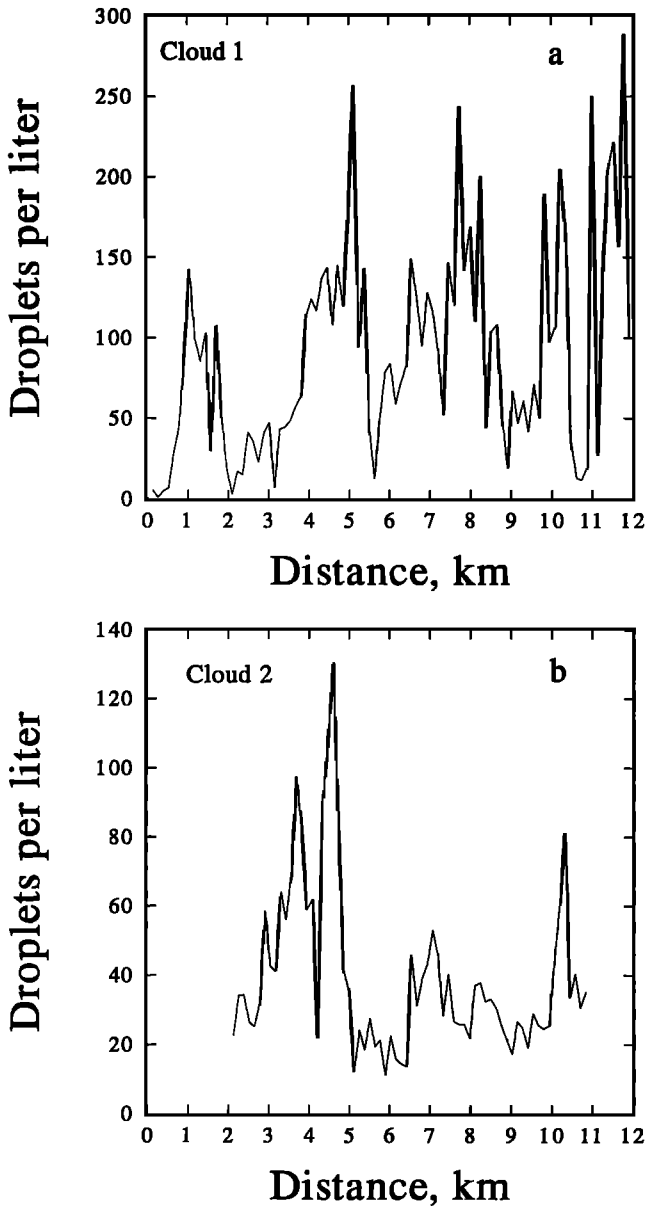


Figure 1. Number of 50 μm diameter cloud droplets per liter measured by the NCAR Electra as a function of distance along a flight path 1 km above cloud base in two different all-liquid tropical oceanic cumulonimbus clouds.

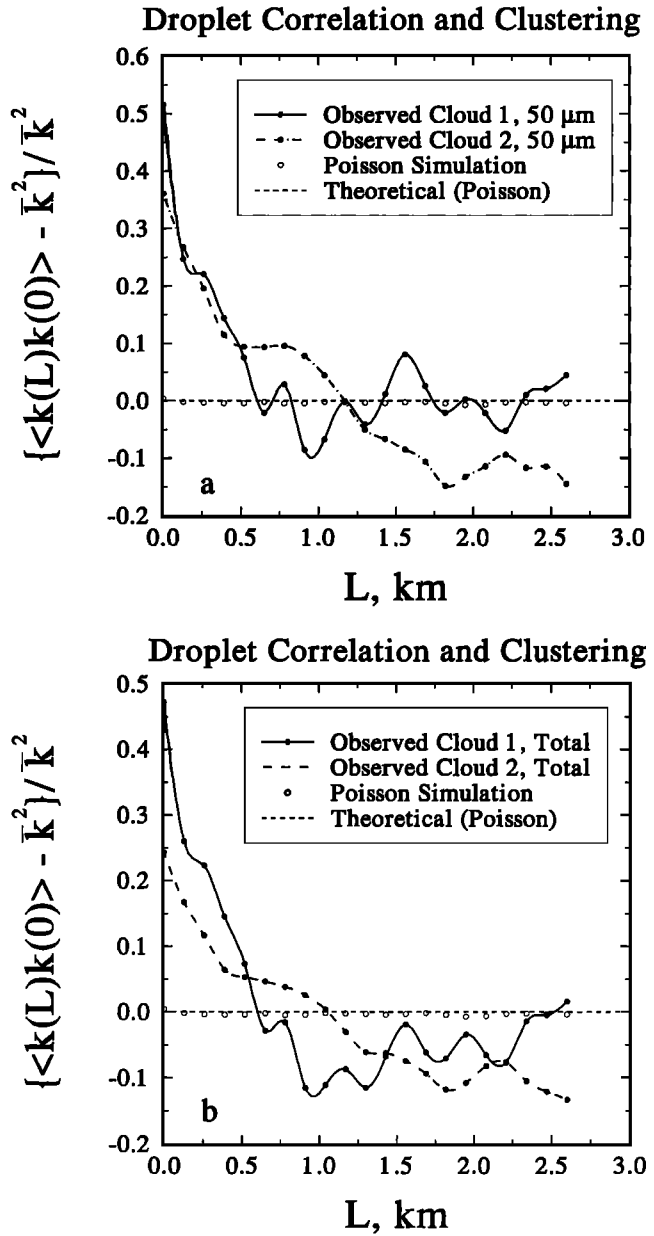


Figure 2. Two-point excess correlation functions for clouds 1 and 2 for lags L for (a) the 50 μm drop sizes and (b) the total number of drops.

the slope and coefficient both equal the inverse of the mean separation.

Histograms of spatial separations of 50 μm drops were measured over an interval of approximately 20 s at a resolution of 0.13 mm in two cumulus clouds, the second corresponding to cloud 2 above. In these cases, however, dead times and the removal of streamers led to occasional artificial contributions to the distribution of separation distances. Consequently, the distributions of data gaps were first determined and compared to the number of droplets occurring in the sequences of buffer outputs. The results are plotted in Figure 4 as functions of the maximum separation distance considered. Obviously, as the maximum distance increases, so does the number of data values and gaps. Thus analyses of these interdrop distances are

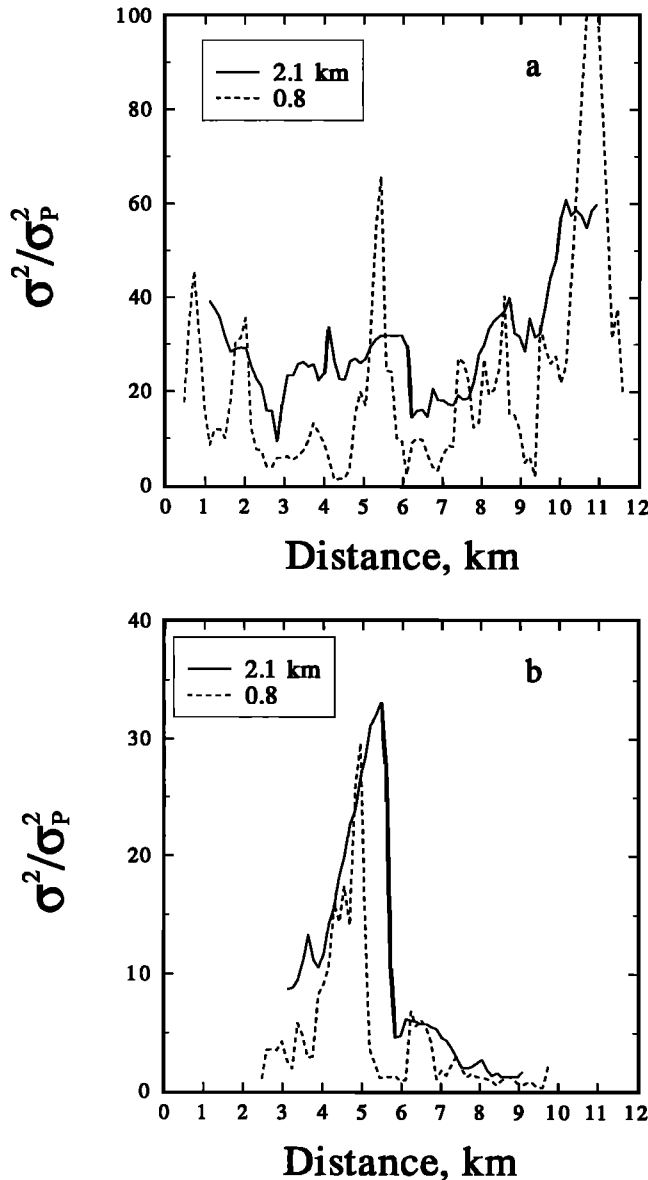


Figure 3. Ratios of the observed variances (σ^2) to those (σ_P^2) for Poisson distributions having the same mean value as observed for $50 \mu\text{m}$ diameter drops using two different sizes of data windows for (a) cloud 1 and (b) cloud 2. The smallest data window contains six data points, while the largest contains 16. If the observations agreed with a Poisson distribution, $\sigma^2/\sigma_P^2 = 1.0$.

restricted to less than or equal to 200 cm in order to avoid any significant data gap contamination.

It is also important to mention that the data segment was carefully selected; so during this entire set of measurements, the total number of observed cloud droplets each second always exceeded a few hundred to several hundred in order to avoid artifacts generated by flying in-between clouds.

Moreover, changes in aircraft airspeed seem unimportant. That is, since $t = \xi/\Gamma$, the variance of the separation times (σ_t^2) is related to the variances of the separation distances (σ_ξ^2) and the aircraft airspeed Γ through

$$\sigma_t^2 = \frac{1}{\langle \Gamma \rangle^2} \sigma_\xi^2 + \langle \xi \rangle^2 \sigma_\Gamma^2 \quad (4)$$

Calculations show that during the 20 s of time series measurements, $\langle \Gamma \rangle = 12,952 \text{ cm s}^{-1}$, $\sigma_{\Gamma/\Gamma}^2 = 6.00 \times 10^{-13}$, $\langle \xi \rangle = 130 \text{ cm}$, $\sigma_\xi^2 \geq \sim 10 \langle \xi \rangle$, so the ratio of the first to the second term is of the order of 760 at most. Hence the fluctuations in aircraft velocity contribute $\leq \sim 0.13\%$ to σ_t^2 . Fluctuations in the aircraft airspeed, while monitored, are inconsequential to these data.

Examples of results are shown in Figure 5. In all cases an exponential function and a power law are fit to these histograms. In addition, the exponential probability density function (pdf) given by (3) is also plotted using the measured mean separation distance ξ_0 . With the one exception in Figure 5a, in most cases and over a wide range of separation limits the exponential fits to the data differ from the exponential pdf associated with a Poisson process. This is illustrated more quantitatively in Figure 6.

In this figure, the slopes and coefficients of the exponential fits to the measurements are compared to the inverse of ξ_0 . The

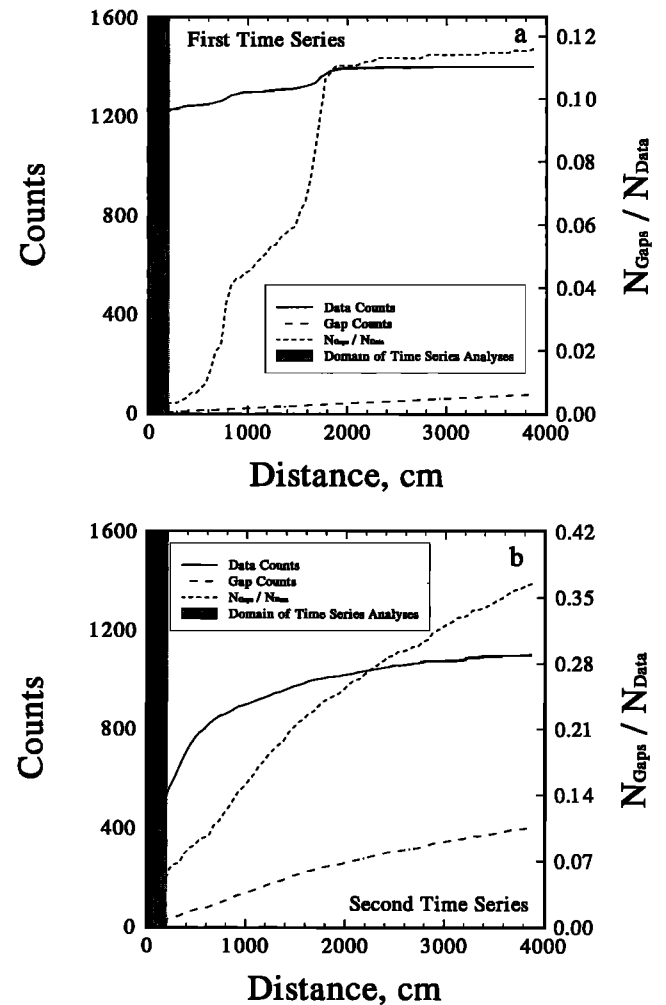


Figure 4. Number of observed $50 \mu\text{m}$ diameter drops and estimates of the number of data gaps as functions of separation limits for the (a) first and (b) second time series. The Poisson distribution would produce a straight line with increasing distance. The shading indicates the domain considered in the subsequent analysis.

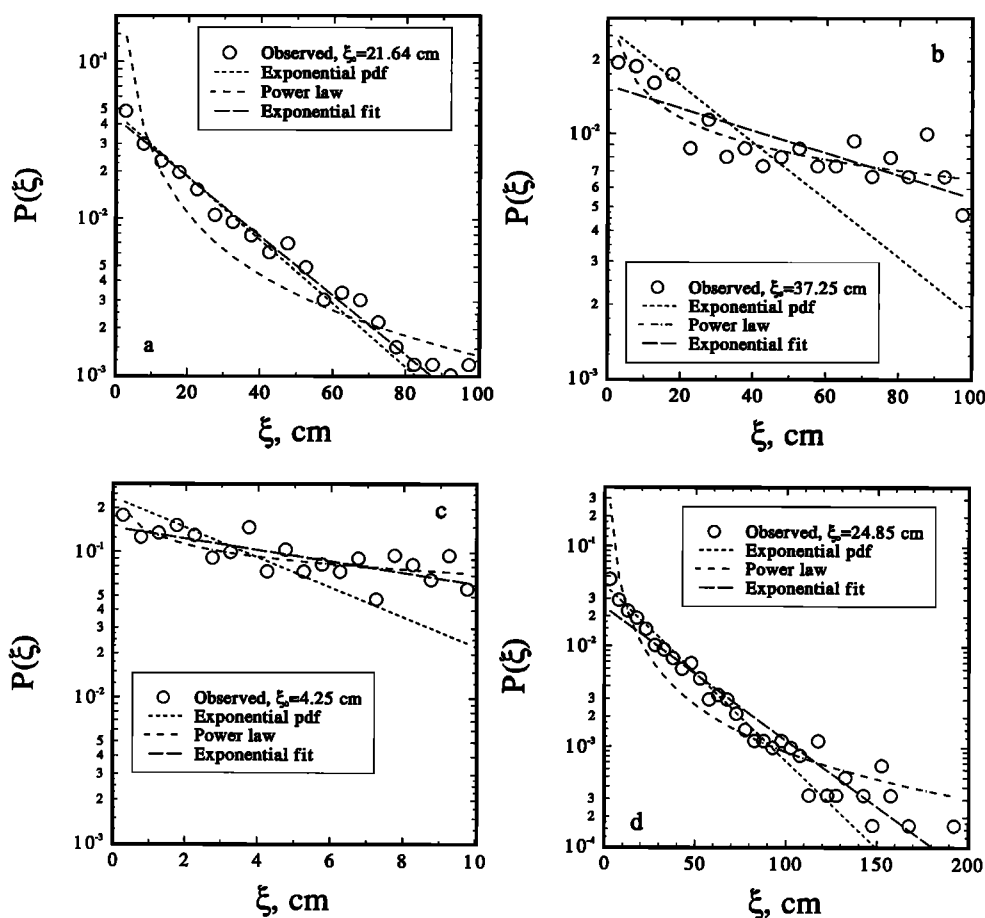


Figure 5. Fits of an exponential function and of a power law to histograms of 50 μm drop time series measurements compared to the exponential pdf expected for a Poisson process having the observed mean separation ξ_0 , corresponding to the separation limits indicated on each axis at the bottom right. Figures 5a, 5c, and 5d are from the first time series, while Figure 5b is from the second time series. Note that while fits of exponential functions are often possible, they do not necessarily correspond to exponential pdfs associated with a Poisson process.

error bars indicate the 95% confidence interval of the observed $1/\xi_0$, while the straight line indicates expectations for a Poisson process, namely, the equality of the slopes, coefficients, and inverse ξ_0 . Generally, for separation limits from 5 to 200 cm the histograms do not match expectations for a Poisson process. There are two exceptions, however, namely, at 100 cm in the first (but not the second) time series and at 5 cm in the second (but not the first) time series. Consequently, we conclude that non-Poisson distributions of cloud droplets appear extensively, although not always exclusively, throughout these data on scales from 200 down to 5 cm.

This detection of clustering appears consistent with measurements by other investigators using an entirely different instrument. Indeed, in cumulus clouds, *Baumgardner et al.* [1993] report 10 cm structures, *Baker* [1992] suggested centimeter structures, while *Paluch and Baumgardner* [1989] observed patchiness over 1–10 m in the upper portions of several cloud turrets of continental cumuli. To quote the latter (pp. 276–277), “In mixed cloud regions there is a high degree of nonuniformity in droplet concentration on a scale of meters or tens of meters.... The small-scale variation in the droplet concentration and the presence of droplet-free regions in mixed cloud volumes do not fit the conceptual model of turbulent mixing as a form of gradient diffusion....”

However, the significance of the work presented here is not simply the reconfirmation of non-Poisson deviations on scales of several centimeters to a few meters already reported by others but rather the detection as well of such deviations over scales from about 100 m to more than 2 km. Moreover, since a Poisson distribution would generate a linear increase in counts with increasing distance, the nonlinear increase of data counts in Figure 4 as well as all the measurements from the second cloud (Figures 2, 3b, and 6b) taken together strongly suggests that non-Poisson deviations are likely occurring simultaneously on many scales from near 5–10 cm up to 2.1 km. In the next section a statistical framework is suggested for describing these deviations.

4. A Statistical Framework Describing Clustering in Clouds

It appears that in these tropical cumulus clouds, deviations from Poisson statistics exist on scales from several centimeters to kilometers. On the basis of the observations in fog, stratocumulus, and stratus clouds mentioned at the beginning of this work, however, it is wise to refrain from too vigorous an extrapolation of such results to all clouds. Nevertheless, for con-

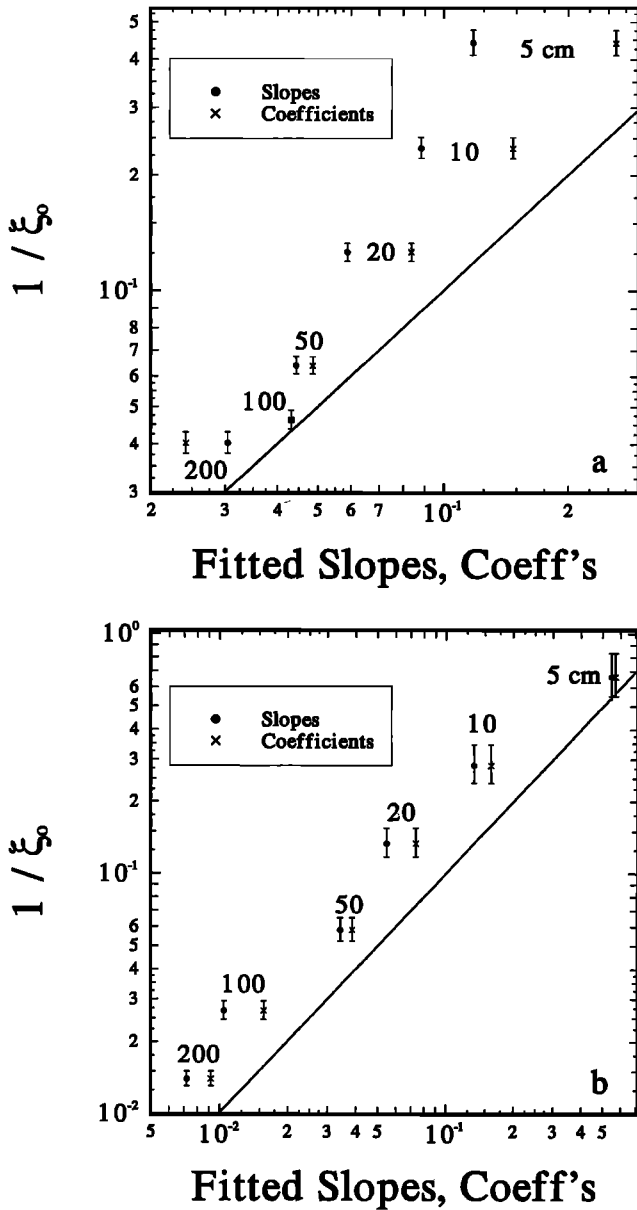


Figure 6. Exponential fits to the histograms for 50 μm drops at each of the indicated separation limits compared to expected values for an exponential pdf corresponding to a Poisson process (straight line) for the (a) first and (b) second time series. Perfect correspondence implies exact equality of the slope, coefficient, and inverse of the measured mean separation distance ξ_0 (see text) along the indicated line. The error bars indicate the 95% confidence interval of the measured $1/\xi_0$. Only for 100 cm in Figure 6a and 5 cm in Figure 6b can the exponential fit be considered an exponential pdf associated with a Poisson process.

vective clouds likely to contain strong turbulence, we propose the following statistical framework for describing clustering.

To begin, consider a minimum temporal resolution of 1 s corresponding to accumulated counts over a minimum sample distance of $x = 130$ m. Figure 2 implies that for 130 m measurements there is a “coherence” distance χ beyond which the droplet counts decorrelate. This coherence distance can be estimated using the autocovariance function given by

$$\text{Cov}\{k(d)k(d+L)\} = \frac{[k(d)k(d+L) - \bar{k}^2]}{\bar{k}^2 - \bar{k}^2} \quad (5)$$

where L is the spatial lag. Figure 7a shows that the $1/e$ coherence distance is about 300–350 m in these two clouds. It is reasonable therefore to define a “cloud patch” corresponding to this distance in a manner analogous to the “rain patch” defined by *Kostinski and Jameson [1997]*. However, it should be noted that the size of the patch (the coherence distance) depends on the minimum resolution x , as Figure 7b illustrates.

There are, then, three important scales involved in counting measurements, namely, the minimum sample resolution x , the total measurement distance X , and the coherence distance χ . Usually, in order to reduce fluctuations, many observations

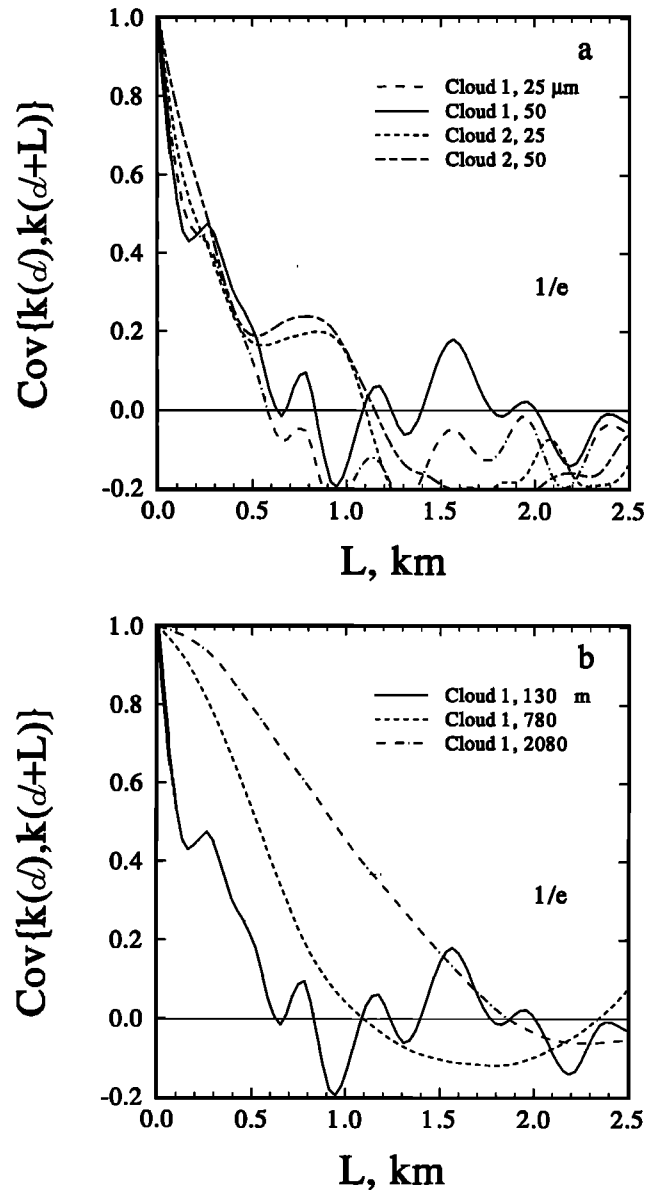


Figure 7. $\text{Cov}\{k(d), k(d+L)\} = \{\langle k(d)k(d+L) \rangle - \langle k \rangle^2\} / \{\langle k^2(d) \rangle - \langle k \rangle^2\}$ for lags L at two different droplet sizes for 130 m data in the two clouds. The $1/e$ coherence distance $\chi \approx 300\text{--}350$ m. (b) Lags for 50 μm drops in cloud 1 show the dependence of χ on measurement resolution x given in the legend.

over x are combined to estimate a mean over X . Whenever $x \ll X \ll \chi$, each sample can be considered to be drawn from a Poisson distribution characterized by the mean over χ . However, whenever $x \ll \chi \ll X$, then like the observations of the clustering of raindrops [Kostinski and Jameson, 1997; Jameson and Kostinski, 1998], the appropriate statistical framework for characterizing droplet counts in variable conditions is likely that of Poisson probability mixtures because the mean value itself now becomes a random variable. The probability density function (pdf) of a particular count over X is then given by

$$P(k) = \int_0^\infty P(k|\bar{k})f(\bar{k})d\bar{k} = \int_0^\infty \frac{\bar{k}^k}{k!}e^{-\bar{k}}f(\bar{k})d\bar{k} \quad (6)$$

where $f(\bar{k})$ is the pdf of the contributing mean values, and the vertical bar denotes conditional probability. The variance of $P(k)$ will be enhanced, sometimes substantially, beyond that of a simple Poisson distribution having the same mean because of the variance of \bar{k} itself (see discussion by Kostinski and Jameson [1997]). Specifically, the variance for such a mixture is given by

$$\sigma_k^2 = E_{\bar{k}}[\sigma^2(k|\bar{k})] + \sigma_{\bar{k}}^2(E[k|\bar{k}]) = \sigma_p^2 + \sigma_{\bar{k}}^2 \quad (7)$$

where the first term is the Poisson variance associated with the global mean given by $\mu = \int_0^\infty \bar{k}f(\bar{k})d\bar{k}$, and the second term is the variance of \bar{k} . Obviously, the variance of k can be significantly increased beyond that of a simple Poisson distribution, as these data suggest. Moreover, it can be shown that (6) implies a mixture of exponential distributions of waiting times (distances) as well.

Specifically, using (6) and rewriting in terms of distance (i.e., $\bar{k} = \xi\nu$), the probability of no droplets occurring ($k = 0$) in distance ξ is given by

$$P(0, \xi) = \int_0^\infty f(\nu)e^{-\nu\xi} d\nu, \nu = \frac{1}{\xi} \quad (8)$$

so that the accumulated probability distribution F that one or more drops occur in ξ is given by

$$F(\xi) = 1 - \int_0^\infty f(\nu)e^{-\nu\xi} d\nu = \int_0^\infty P(\xi) d\xi \quad (9)$$

Taking the derivative of $F(\xi)$ with respect to ξ , it follows that

$$P(\xi)d\xi = \int_0^\infty \nu f(\nu)e^{-\nu\xi} d\nu \quad (10)$$

That is, for a Poisson probability mixture, the waiting distances (times) are a probability mixture of the exponential waiting distances (times) associated with each Poisson distribution contributing to (6).

As two examples, Kostinski and Jameson [1997] show that if $f(\bar{k})$ were an exponential distribution, $P(k)$ would become the geometric distribution given by

$$P(k, \mu) = \frac{1}{1 + \mu} \left(\frac{\mu}{1 + \mu} \right)^k \quad (11)$$

where μ is the ‘‘global’’ average over $f(\bar{k})$. For waiting distances (times) the integration of (10) for the corresponding exponential distribution of $f(\nu)$ yields

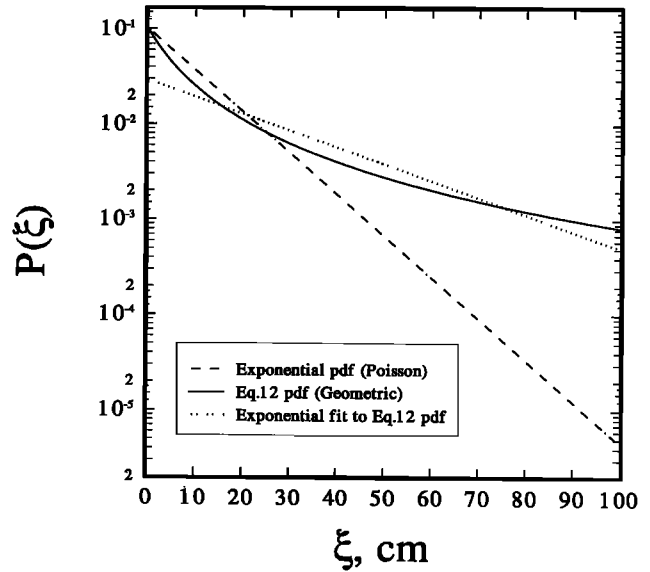


Figure 8. Probability density function of separation distances $P(\xi)$ corresponding to a Poisson [exponential $P(\xi)$] and to a geometric [$P(\xi)$ given by equation (12)] distribution of drops. The $P(\xi)$ for the geometric distribution representing clustering is enhanced compared to that for a Poisson $P(k)$, consistent with the data and curves in Figure 5.

$$P(\xi)d\xi = \frac{1}{\xi_0 \left(\frac{\xi}{\xi_0} + 1 \right)^2} d\xi \quad (12)$$

This expression depends only on ξ and ξ_0 , the global average of ξ .

On the other hand, if $f(\bar{k})$ were a gamma distribution, $P(k)$ would become the negative binomial distribution given by

$$P(k, \mu, m) = \binom{k + m - 1}{k} \left(\frac{m}{m + \mu} \right)^m \left(\frac{\mu}{m + \mu} \right)^k \quad (13)$$

while for the corresponding gamma distribution of $f(\nu)$

$$P(\xi)d\xi = \frac{m}{\xi_0 \left(\frac{\xi}{\xi_0} + 1 \right)^{m+1}} d\xi \quad (14)$$

where m is a parameter that can be adjusted so that the variance of P matches the observed variance of a data set (for measured mean μ and variance σ^2 , $m = \text{int}[(1/p)(\mu^2/\sigma^2)]$ where $p = 1 - (\mu/\sigma^2)$ and int is the integer function [see Ochi, 1990, p. 96]).

To illustrate, $P(\xi)$ given by (12) is plotted in Figure 8 along with the exponential pdf corresponding to the Poisson $P(k)$ having the same mean separation. In addition, there is also a plot of an exponential fit to $P(\xi)$ for the geometric distribution of $P(k)$. The general features of Figure 8 are remarkably similar to the plots in Figure 5. That is, the exponential pdf falls off much more quickly with increasing distance than does the pdf when the drops are clustered. This is also reflected in the flatter slope of the exponential fit to the pdf (12) corresponding to the geometric distribution $P(k)$.

It must be remembered, however, that we do not really know the exact form of $P(k)$ corresponding to the measurements (Figure 5). It is not surprising then that neither (12) nor (13),

based on assumed theoretical $P(k)$, match the data precisely. However, even without knowing $P(k)$, Figure 8 nevertheless captures the essential features evident in the data, indicating that the measurements are consistent with the clustering of the drops.

A different, complementary tact is to use the total number of droplets detected by the 2DC-PMS cloud probe over all 32 bins (25–800 μm diameter) rather than drops only of one size. If the different counts at different sizes are uncorrelated and if none dominate the sum (i.e., under conditions quite similar to those for the Central Limit Theorem), then statistical theory [Kovalenko *et al.*, 1996, p. 163] shows that a sum of independent random counts tends toward a Poisson distribution regardless of the underlying probability density functions of the individual components. Hence if clouds were described by M independent droplet counts at M different sizes corresponding to each of the PMS probe bins, the statistics of the sum total should approach a Poisson distribution.

As Figure 9 illustrates, however, neither the distributions nor the variances are Poisson. Indeed, the histogram for cloud 1 is well approximated by either a geometric distribution corresponding to the mean 425.59 counts or a negative binomial distribution having the same mean with parameter $m = 2$. On the other hand, cloud 2 is best approximated by a negative binomial having a mean of 161.11 counts and $m = 4$. While it cannot be claimed that these results “prove” the applicability of the Poisson mixture (6) to these data, the results in Figure 9 (and indeed Figure 2 as well) suggest the presence of correlations consistent with such a formulation. Aside from this consideration these results emphasize that care must be taken to assure that $x \ll X \ll \chi$ in order to avoid mixing counts from different cloud patches and thereby enhancing statistical uncertainty of the measured mean droplet concentration.

5. Discussion

Using a variety of analysis tools, measurements in two tropical cumulus clouds indicate that droplet clustering is occurring on many scales. Specifically, the two-point excess correlation function shows clustering occurring over scales from about 100 m up to 1 km or more, while an analysis of interdrop distances suggest clustering from several centimeters to tens of meters, consistent with previous studies.

These particular scales of clustering are important. At the longer end and for a cloud of droplets of one size, the mean free path of a photon λ is inversely proportional to the product of droplet concentration times the particle-scattering cross section (for example, see Reif [1965, pp. 463–471] for a kinematic analogy in ideal gases). The importance of clustering is that λ can vary considerably throughout a cloud, thereby perhaps altering the overall radiation properties of the cloud from those of an equivalent (mean sense) Poisson cloud, as Cahalan *et al.* [1994] suggest.

At the smaller scale of centimeters, clustering may alter the environment for droplet growth from that anticipated for a Poissonian cloud. For example, both Paluch and Baumgardner [1989] and Cooper [1989] consider the effects on droplet growth through condensation associated with fluctuations in saturation occurring from the mixing of cloudy and entrained air. Here we emphasize that super-Poissonian concentration fluctuations associated with clustering may significantly enhance drop growth through coalescence, as originally suggested by Telford [1955] and Twomey [1964].

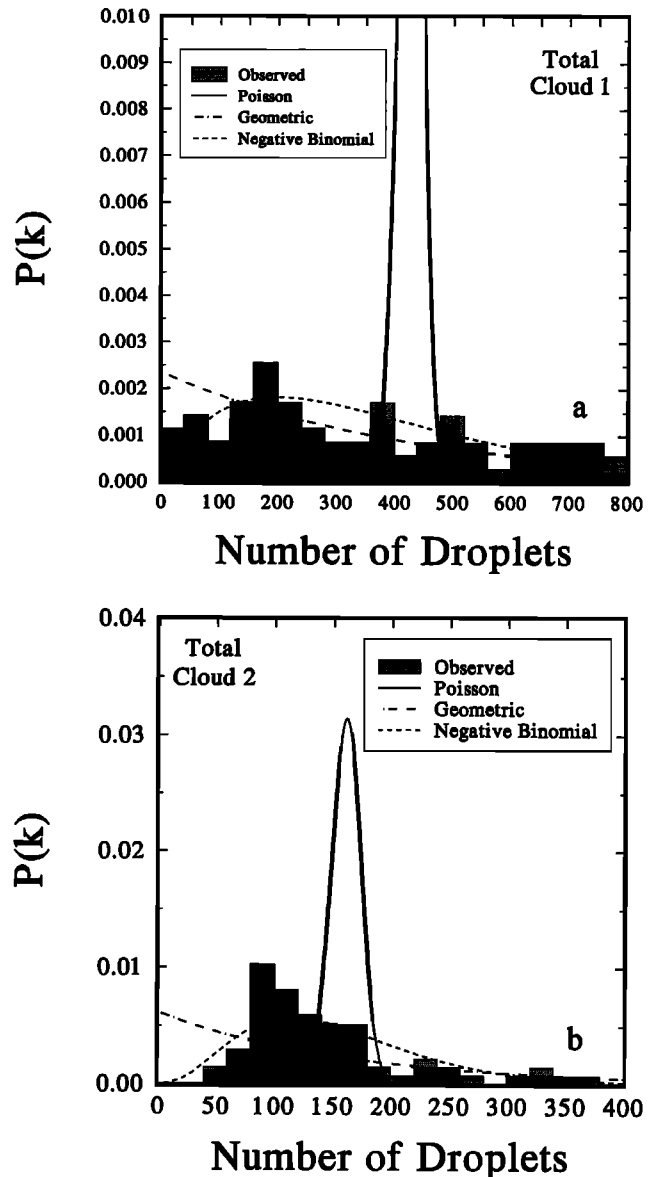


Figure 9. Histograms of the total number of 25–800 μm diameter drops measured in (a) cloud 1 ($\mu = 425.59$, $\sigma^2 = 86517$) and (b) cloud 2 ($\mu = 161.11$, $\sigma^2 = 6406.9$) compared to three different distributions discussed in the text.

While these ideas are obviously only speculations at this point, the results of this study suggest that it may now be time to begin considering the potential role of detailed cloud structure on scales of a few kilometers and smaller. The analyses in this work suggest a framework for statistically characterizing such structure for future detailed calculations and simulations.

Acknowledgments. Support for this work was provided by the National Science Foundation under grants ATM95-12685 (ABK), ATM97-08657 (ARJ), and ATM94-19523 (ARJ). Support for R. Black came from the National Oceanic and Atmospheric Administration through the Atlantic Oceanographic and Meteorological Laboratory.

References

Baker, B. A., Turbulent entrainment and mixing in clouds: A new observational approach, *J. Atmos. Sci.*, 49, 387–404, 1992.

- Baumgardner, D., A new technique for the study of cloud microstructure, *J. Atmos. Oceanic Technol.*, **3**, 340–343, 1986.
- Baumgardner, D., B. Baker, and K. Weaver, A technique for the measurement of cloud structure on centimeter scales, *J. Atmos. Oceanic Technol.*, **10**, 557–565, 1993.
- Cahalan, R. F., Overview of fractal clouds, in *Advances in Remote Sensing Retrieval Methods*, edited by A. Deepak, H. E. Fleming, and J. S. Theon, pp. 371–389, A. Deepak, Hampton, Va., 1989.
- Cahalan, R. F., W. Ridgway, W. J. Wiscomb, and T. L. Bell, The albedo of fractal stratocumulus clouds, *J. Atmos. Sci.*, **51**, 2434–2455, 1994.
- Cooper, W. A., Effects of variable droplet growth histories on droplet size distributions, I, Theory, *J. Atmos. Sci.*, **46**, 1301–1311, 1989.
- Cornford, G. S., Sampling errors in measurements of raindrop and cloud droplet concentration, *Meteorol. Mag.*, **96**, 271–282, 1967.
- Feller, W., *An Introduction to Probability Theory and Its Applications*, vol. 1, 478 pp., John Wiley, New York, 1968.
- Gillespie, D. N., The stochastic coalescence model for cloud droplet growth, *J. Atmos. Sci.*, **29**, 1496–1510, 1972.
- Gillespie, D. N., Three models for the coalescence growth of cloud drops, *J. Atmos. Sci.*, **32**, 600–607, 1975.
- Jameson, A. R., and A. B. Kostinski, Fluctuation properties of precipitation, II, Reconsideration of the meaning and measurement of raindrop size distributions, *J. Atmos. Sci.*, **55**, 283–294, 1998.
- Knollenberg, R. G., Clouds: Their optical properties and effects, in *Techniques for Probing Cloud Microstructure*, edited by P. V. Hobbs and A. Deepak, pp. 15–89, Academic, San Diego, Calif., 1981.
- Kostinski, A. B., and A. R. Jameson, Fluctuation properties of precipitation, I, On deviations of single-size drop counts from the Poisson distribution, *J. Atmos. Sci.*, **54**, 2174–2186, 1997.
- Kovalenko, I. N., N. Y. Kuznetsov, and V. M. Shurenkov, *Models of Random Processes: A Handbook for Mathematicians and Engineers*, 446 pp., CRC Press, Boca Raton, Fla., 1996.
- Kozikowska, A., K. Haman, and J. Supronowicz, Preliminary results of an investigation of the spatial distribution of fog droplets by a holographic method, *Q. J. R. Meteorol. Soc.*, **110**, 65–73, 1984.
- Ochi, M., *Applied Probability and Stochastic Processes*, 499 pp., John Wiley, New York, 1990.
- Paluch, I. R., and D. Baumgardner, Entrainment and fine-scale mixing in a continental convective cloud, *J. Atmos. Sci.*, **46**, 261–278, 1989.
- Peebles, P. J. E., *The Large-Scale Structure of the Universe*, 422 pp., Princeton Univ. Press, Princeton, N. J., 1980.
- Pruppacher, H. R., and J. D. Klett, *Microphysics of Clouds and Precipitation*, 954 pp., Kluwer Acad., Norwell, Mass., 1997.
- Ramanathan, V., B. Subasilar, G. J. Zhang, W. Conant, R. D. Cess, J. T. Kiehl, J. T. Grassal, and L. Shi, Warm pool heat budget and short wave cloud forcing: A missing physics?, *Science*, **267**, 499–503, 1995.
- Reif, F., *Fundamentals of Statistical and Thermal Physics*, 651 pp., McGraw-Hill, New York, 1965.
- Rogers, R. R., and M. K. Yau, *A Short Course in Cloud Physics*, 229 pp., Pergamon, Tarrytown, N. Y., 1989.
- Telford, J. W., A new aspect of coalescence theory, *J. Meteorol.*, **12**, 436–444, 1955.
- Twomey, S., Statistical effects in the evolution of a distribution of cloud droplets by coalescence, *J. Atmos. Sci.*, **21**, 553–557, 1964.
- van Kampen, N. G., *Stochastic Processes in Physics and Chemistry*, 465 pp., North-Holland, New York, 1992.
- Young, K. C., *Microphysical Processes in Clouds*, 427 pp., Oxford Univ. Press, New York, 1993.

R. A. Black, National Oceanic and Atmospheric Administration, Atlantic Oceanographic and Meteorological Laboratory, Miami, FL 33149.

A. R. Jameson, RJH Scientific, Inc., 5904 Richmond Hwy., Ste 401, Alexandria, VA 22303. (e-mail: jameson@rjhsci.com)

A. B. Kostinski, Department of Physics, Michigan Technological University, Houghton, MI 49931.

(Received April 4, 1997; revised January 5, 1998; accepted January 5, 1998.)